J Mol Model (2005) 11: 341–350
DOI 10.1007/s00894-005-0253-x

ORIGINAL PAPER

Mariusz Mitoraj · Artur Michalak

DFT studies on isomerization reactions in the copolymerization of ethylene and methyl acrylate catalyzed by Ni-diimine and Pd-diimine complexes

Received: 28 October 2004 / Accepted: 31 January 2005 / Published online: 4 May 2005

Abstract Gradient corrected density functional theory (DFT) has been used to investigate the isomerization reactions in the process of the ethylene/methyl acrylate copolymerization catalyzed by Pd-dimine and Ni-dimine complexes, modeled by a generic system N∧N–M–$(CH_3)^+$; N∧N = –N(H)-C(H)-C(H)-N(H)-. The influence of the polar group and of the metal on the isomerization mechanism was studied. The results show that for the Pd-catalyst the isomerization follows the standard mechanism observed in homopolymerization processes, with the β-hydrogen-transfer to the metal and formation of a π-olefin–hydride complex. Electron withdrawing character of the polar group results in an increase of the hydride energy and the isomerization barrier. For the Ni-catalyst the overall isomerization picture is modified by the formation of a σ-olefin–hydride complex, in which the olefin is coordinated to the metal by the oxygen atom of the polar group. Such a σ-olefin–hydride is lower in energy for the Ni catalyst than the π-olefin–hydride complex by 9.6 kcal mol^{-1} . The latter is preferred by 2.6 kcal mol^{-1} for the Pd-based system. The calculated isomerization barriers are 20.9 and 24.0 kcal mol^{-1} (with respect to the initial 4-member chelate) for the Pd-catalyst and Ni-catalyst, respectively. This can result in a larger fraction of ester group directly connected to the copolymer backbone observed experimentally for the Ni-catalyst.

Keywords Single-site olefin polymerization · Polar copolymerization · Chain isomerization · Mechanism · Diimine catalysts

M. Mitoraj · A. Michalak (✉)
Department of Theoretical Chemistry,
Faculty of Chemistry,
Jagiellonian University,
R Ingardena 3, 30-060 Cracow, Poland
E-mail: michalak@chemia.uj.edu.pl

Introduction

During last decade there has been an increasing interest in employing late-transition-metal complexes as catalysts for α-olefin polymerization processes [1–5], leading to a development of new catalytic systems not only capable of polymerizing ethylene, but also active in copolymerization of olefins with monomers bearing polar-groups [2, 6]. The first successful example of a single-site catalyst for the ethylene-methyl acrylate copolymerization process was a family of palladium complexes with bulky α-diimine ligands [2, 7, 8] introduced earlier as oligomerization and homopolymerization catalysts [2, 9, 10]. In both, homo-polymerization and co-polymerization processes, these systems produce polymers with unique microstructures, varying from linear to hyper branched topologies. The polymer branching/topology can be controlled by the reaction conditions (*T, p*) and the catalyst substituents [2, 11–16].

The mechanism of the α-olefin polymerization and co-polymerization with polar monomers is shown in Fig. 1. The initial active form of the catalyst is an alkyl complex **1**. In the standard Cossee–Arlman mechanism [17, 18] of the α-olefin polymerization a monomer insertion (Fig. 1a) follows complexation of an olefin by its double C = C bond (π-complex, **2**). Similarly, in a polar copolymerization process the polar monomer can form a corresponding π-complex, **2A**. However, a σ-complex (**2A'**) can alternatively be formed, with a polar molecule bound by an atom of its functional group, e.g. the carbonyl oxygen in the case of acrylates. A competition between the two binding modes of polar olefins is an important factor for the catalyst activity, as insertion of the polar monomer in such a random copolymerization mechanism can exclusively start from the π-complex, whereas formation of a too stable σ-complex poisons the catalyst. In the case of diimine complexes, it has been found [19, 20] that for the Ni-diimine systems the σ-binding mode is preferred by ca. 3 kcal mol^{-1}, while the π-complex has lower energy for the Pd-based

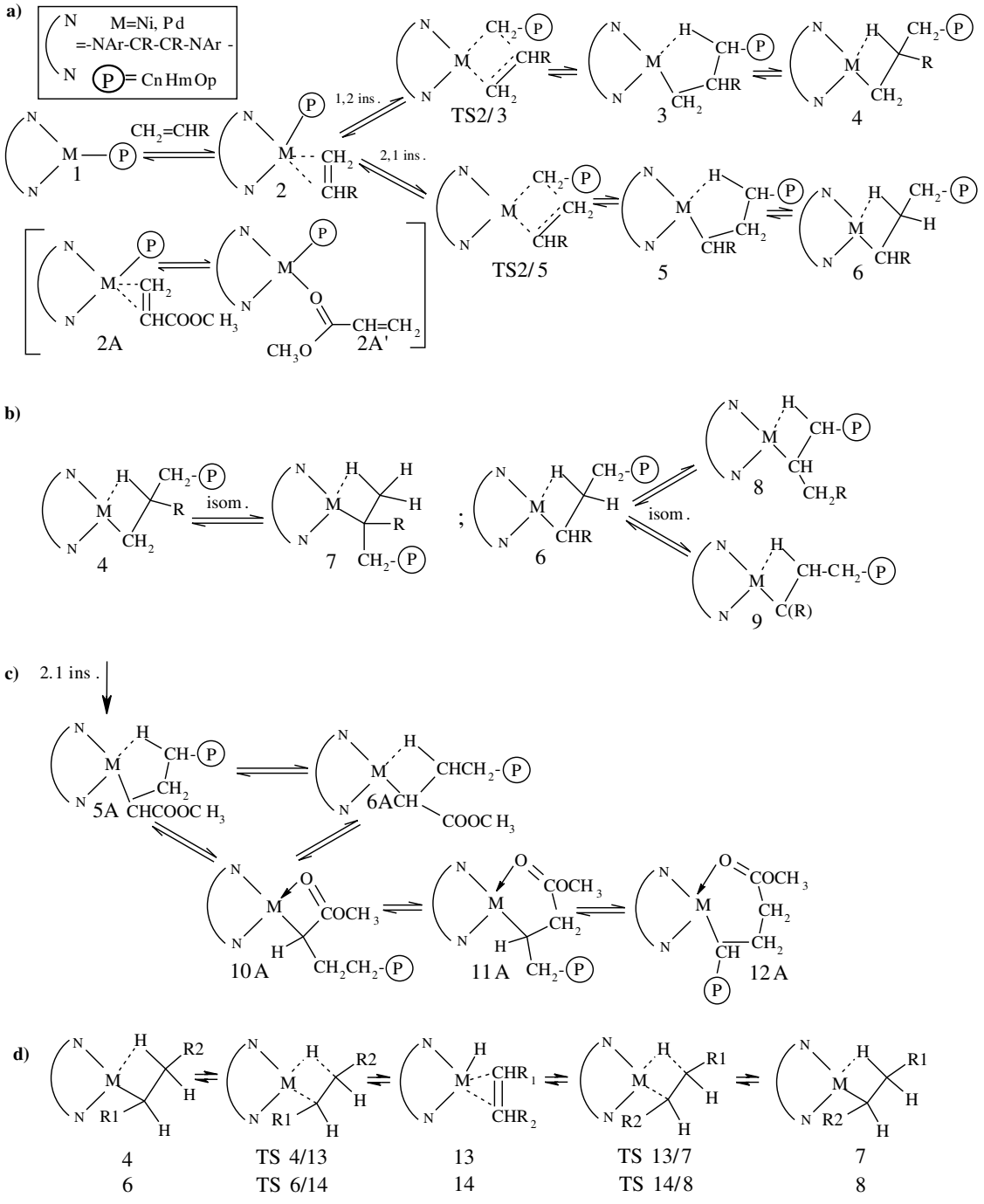

Fig. 1 Mechanism of α-olefin polymerization and polar copolymerization processes catalyzed by diimine complexes: chain propagation steps (a), chain isomerization steps (b), chelate formation steps (c), and details of the isomerization mechanism (d)

catalysts. The mechanism for monomer insertion is similar for polar and non-polar olefin. In general, two insertion pathways, 1,2-insertion (**2** → TS-2/3 → 3 → 4) and 2,1-insertion (**2** → TS-2/5 → 5 → 6), are possible for higher olefins; for ethylene they become identical. The 2,1-insertion is usually electronically preferred in the processes catalyzed by the late-transition-metal systems [19, 21, 22] but steric factors favor the 1,2-insertion [19, 22]. The γ-agostic alkyl complexes (**3** and **5**) are the kinetic insertion products. They can easily isomerize to form more stable β-agostic species (**4** and **6**).

The β-agostic alkyl complexes can capture and insert the next monomer molecule, again following the mechanism of Fig. 1a (**1** → 4 or 1 → 6). However, in many polymerization processes catalyzed by the late-metal complexes, the isomerization reactions occur in addition (Fig. 1b). The isomerization reactions influence polymer branching. They introduce branches of variable length in polyethylenes, and remove/shorten the branches in

higher polyolefins. For example, isomerization directly following the 1,2-olefin insertion (**4** → 7, see Fig. 1b) introduces an additional methyl branch, while the reactions directly following the 2,1-insertion may either elongate (**6** → 8), or shorten/remove (**6** → 9) the existing branch. Fast 'chain walking', which proceeds by subsequent isomerizations, is responsible for unique polymer microstructures observed in many processes, e.g. those catalyzed by the diimine-catalysts [2, 11–16]. The standard isomerization mechanism is shown in Fig. 1d. It involves the β-hydrogen abstraction from 4 or 6, to form an intermediate olefin hydride complex (**13** or **14**). An olefin rotation followed by reinsertion of hydrogen leads to an isomeric β-agostic product (**7**or **8**).

In the case of polar monomer insertion, the agostic species isomerizes further to form more stable chelates, with a strong metal-polar atom (e.g. oxygen) bond (Fig. 1c). For example, after the 2,1-insertion of methyl acrylate, the 4-membered chelate (**10A**) can be formed from the agostic species (**5A** and **6A**). Subsequent isomerization reactions can lead to the 5-membered and 6-membered chelates. It has been observed experimentally [7, 8], and shown by theoretical calculations [23, 24] that the 5-membered (**11A**) and 6-membered (**12A**) chelates are the most stable species in the catalytic cycles with the Ni-diimine and Pd-diimine complexes. It should be pointed out that isomerization reactions following the polar monomer insertion influence the positions of the ester groups in the resulting copolymer structure. Namely, ethylene insertion directly following formation of the 4-member chelate results in a structure with the $-COOCH_3$ group linked to the polymer backbone. If a 5-member/6-member chalate is formed prior to the ethylene insertion then the ester group is separated by one/two $-CH_2$-groups from the chain. Predominantly in-chain acrylate incorporation was observed experimentally for Ni-catalysts [25] while for Pd-based systems the ester groups occur largely at the ends of branches [2, 7, 8, 25].

The major goal of the present study is to investigate by theoretical calculations the details of the isomerization reactions in the ethylene-methyl acrylate copolymerization catalyzed by the Pd-diimine and Ni-diimine catalysts. There exist numerous theoretical studies of the chain propagation, termination, and isomerization reactions in α-olefin homopolymerization processes catalyzed by the transition-metal-based systems [26–28]. For polar copolymerization processes, the mechanism of the chain propagation reactions has been investigated by static and dynamic DFT calculations [23, 24, 29–32]. However, the isomerization reactions in the polar copolymerization processes have not been studied. In particular, it is important whether the isomerizations between alternative chelates (**10A** → 11A → 12A, see Fig. 1c) follow the same route as in homopolymerization (with agostic intermediates; Fig. 1d), or if the presence of a polar group modifies the mechanism. In the following, a comparison of the isomerization mechanism with and without the polar group will be presented, together with a comparison of the metal influence (Pd versus Ni). Gradient corrected density functional theory (DFT) was used in the present study. The DFT approach is now well established as a valuable tool for studying electronic structure and the reactions involving transition-metal complexes [33–36] including polymerization processes [19–32].

Computational details and the model systems

The reactions and complexes studied in the present work are shown in Fig. 2. For clarity, the species are labeled as in Fig. 1, with the letter A or E added for those formed after acrylate and ethylene insertion, respectively. In addition, in the text and tables the species formed with palladium and nickel-based catalyst will be identified by a suffix **–Pd** and **–Ni**, respectively, e.g. **10A-Pd** and **10A-Ni**. In the present study the cationic diimine catalyst was modeled by a *generic* $N\wedge N–M^+$ complex, with M = Ni, Pd, and N∧N = –NHCHCHNH–, in which the bulky substituents of the real catalysts were replaced by hydrogen atoms. It has been found previously that the catalyst substituents have minor influence on the isomerization reactions in the ethylene homopolymerization [21, 22].

It can be expected that the isomerization reaction between 4-membered and 5-membered chelates formed after 2,1-acrylate insertion, **10A** and **11A** (Fig. 2), can proceed with formation of an intermediate agostic species, **6A** and **8A**, and with the standard isomerization mechanism (Fig. 1d) involving olefin–hydride species, **14A**. Such an isomerization mechanism assumes practically no participation of the acrylate polar group once the agostic species **6A** and **8A** are formed. Alternatively, on the pathway leading from chelates **10A** and **11A** to agostic complexes **6A** and **8A**, intermediate structures can hypothetically exist, in which both the agostic, M–H and chelating M–O bonds are present. If such structures existed on the potential energy surface, the isomerization between chelates **10A** and **11A** could proceed with the metal–oxygen bond present along the whole isomerization pathway. Therefore, we investigated the pathways leading from chelates **10A** and **11A** to agostic structures **6A** and **8A**, respectively. This was studied by linear-transit reaction-path calculations, with the torsion angles defining rotation around the $M–C_\alpha$ and $C_\alpha–C_\beta$ bonds used as reaction coordinates for **10A** ↔ **6A** and **8A** ↔ **11A** isomerizations, respectively. Further, the pathways corresponding to the standard isomerization mechanism between the agostic species **6A** and **8A**, with an intermediate hydride **14A**, were studied and compared with the corresponding pathways present in the ethylene homopolymerization process, **6E** ↔ 14E ↔ 8E (Fig. 2b). Finally, in the case of polar monomer, an additional structure of the hydride complex can occur, with σ-bound acrylate, **14A**'. Therefore, the geometry of such a species and the corresponding isomerization pathways **6A** ↔ 14A'↔ 8A were also studied.

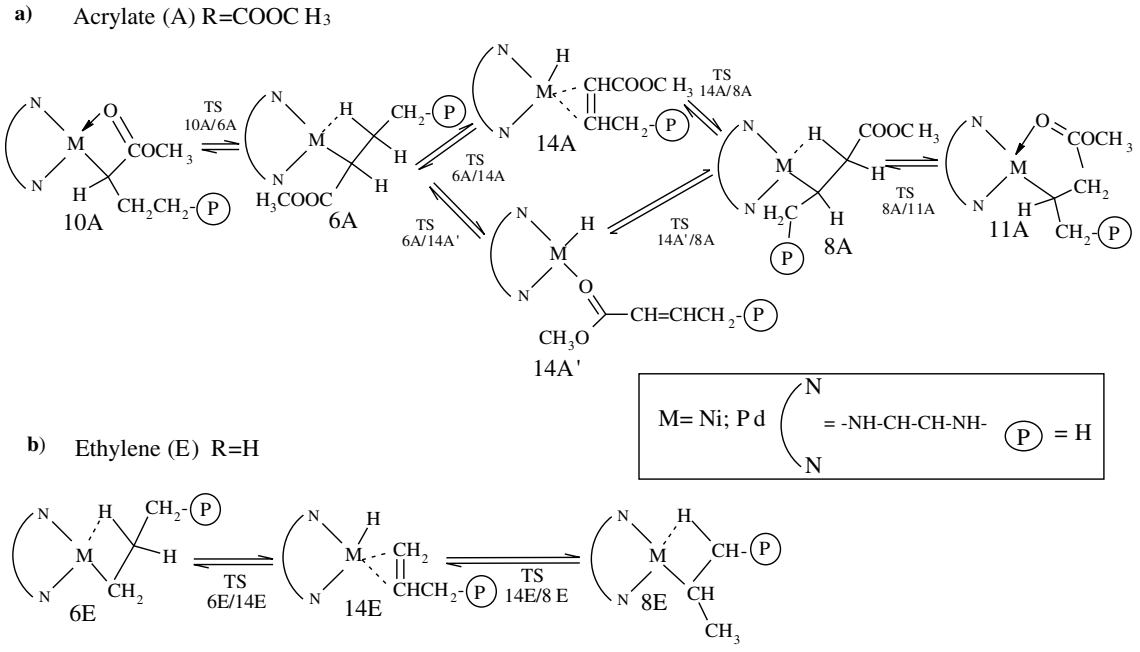

Fig. 2 Reactions and complexes studied in the present article:

The DFT calculations based on the Becke–Perdew exchange-correlation functional [37–39] were performed using the Amsterdam Density Functional (ADF) program, Version 2003.01 [40–45]. A standard double-zeta STO basis with one set of polarization functions was used for H, C, N, and O atoms, while a standard triple-zeta basis set was used for the Ni and Pd atoms. The *1s* electrons of C, N, O as well as the *1s-3d* electrons of Pd and the *1s-2p* electrons of Ni were treated as frozen core. Auxiliary *s, p, d, f*, and *g* STO functions, centered on all nuclei, were used to fit the electron density and obtain accurate Coulomb and exchange potentials in each SCF cycle. The reported energy differences include a first-order scalar relativistic correction, [46–48] since it has been shown that such an approach is sufficient for *4d* transition metal atoms [49]. The Nalewajski–Mrozek bond order analysis [50–54] and the Ziegler–Rauk bond-energy decomposition [55, 56] were also used.

Results and discussion

Isomerization reactions with the Pd-based diimine catalyst

The energy profile for isomerization pathways in the co-polymerization process catalyzed by the Pd-diimine complexes is summarized in Fig. 3, together with the structures of the reactants, products and the reaction intermediates. The geometries shown in Fig 3 clearly indicate that in the case of polar copolymerization isomerization pathways directly corresponding to those of α-olefin homopolymerization exist, i.e. the polar group does not directly participate in the reaction. In the structures of the *β*-agostic complexes **6A-Pd** and **8A-Pd**, in the olefin–hydride intermediate **14A-Pd**, as well as in the corresponding transition states (**6A/14A** and **14A/8A**) there are no metal–oxygen bonds.

The presence of the polar group, however, does affect the energy profile of the process. The relative energies of the structures involved in the reactions with and without polar group are compared in Table 1. The results show that the polar group affects the relative stability of the isomeric agostic complexes **6A-Pd** and **8A-Pd**, compared to **6E-Pd** and **8E-Pd**. Further, it increases the energy of the intermediate hydride complex **14A-Pd**, compared to **14E-Pd**, and the activation barriers of the isomerization.

In order to facilitate the discussion of the polar-group effect, Table 2 lists the crucial interatomic distances and the corresponding bond-order values in the agostic complexes **6A-Pd** and **8A-Pd**. Let us first discuss the relative stability of the agostic complexes **6A-Pd** and **8A-Pd**. It follows from Table 2 that the destabilization of **8A-Pd** compared to **6A-Pd** is due to weakening of the Pd–H agostic interaction and strengthening of the C_β–H bond: the Pd–H bond is slightly longer in **8A-Pd** (1.77 Å) than in **6A-Pd** (1.74 Å), and the C_β–H bond is shortened in **8A-Pd** compared to **6A-Pd** (1.21 Å vs. 1.23 Å). The corresponding bond-order values reflect the trend observed in bond lengths. For Pd–H they are 0.13, and 0.14, and for C_β–H: 0.74 and 0.73, in **8A-Pd** and **6A-Pd**, respectively. This effect can be attributed to the electron-withdrawing effect of the polar group, which is more pronounced in **8A-Pd**, because in this structure the polar group is closer to the atoms participating in the agostic bond C_β–H–Pd.

The results shown in Fig. 3 and Table 1 demonstrate that the presence of the polar group destabilizes the

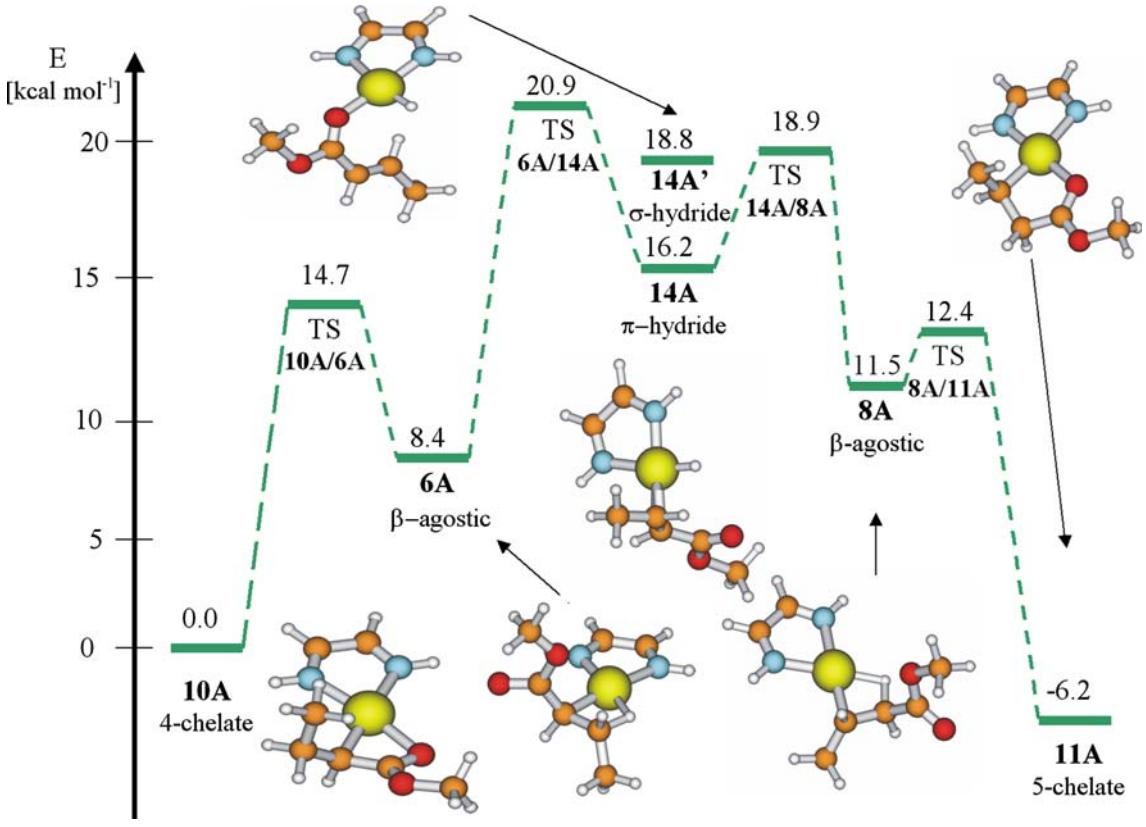

Fig. 3 Energy profile and the crucial structures for the isomerization reactions in the process catalyzed by the Pd-diimine complex. Energies are in kilocalories per mole, structure labeling as in Fig. 2

hydride complex, **14A-Pd**, compared to the corresponding structure in homopolymerization, **14E-Pd**. As in the previous paragraph, this can be explained in terms of the bond-length/bond-order trends in agostic complexes. Namely, the C_β–H bond is shorter in **6A-Pd** (1.23 Å) than in **6E-Pd** (1.25 Å), and the Pd–H bond is longer (1.74 Å vs. 1.72 Å, in **6A-Pd** in **6E-Pd**, respectively). This is reflected by the corresponding bond-order values: 0.73 and 0.71 for C_β–H bond, and 0.14 and 0.15 for Pd–H bond, in **6A-Pd** and **6E-Pd**, respectively. Thus, the β-hydrogen transfer to the metal resulting in formation of **14A-Pd** is more difficult in the case of **6A-Pd**, compared to **6E-Pd**. Again, this effect comes as a result of the electron-withdrawing character of the polar group. To validate the conclusions presented above further by estimation of the C_β–H and Pd–C_α bond-energies, the calculations were performed for two dissociation reactions shown in Fig. 4, i.e. breaking both of the bonds discussed (Fig. 4a), and breaking the agostic Pd–H bond only (Fig. 4b). The results show that the first reaction requires 84.8 kcal mol^{-1} for **6A-Pd** and 82.9 kcal mol^{-1} for **6E-Pd**. The agostic bond-breaking energy is 11.7 kcal mol^{-1} in **6A** and 16.9 kcal mol^{-1} in 6E. These results confirm the conclusions drawn from the bond length/bond-order data.

Finally, we would like to discuss a possibility of an alternative isomerization mechanism with direct participation of the polar group, i.e. with the Pd–O bond present along the whole isomerization pathway. A necessary condition for such a pathway to be facile is a simultaneous presence of both the agostic Pd–H, and chelating Pd–O bond. Figure 5a shows the energy profile for the first step in the process in question, i.e. the isomerization reaction between the agostic complex **6A-Pd** and the chelate **10A-Pd**. Figure 5b shows the Pd–H (agostic) and Pd–O (chelating) interatomic-distance

Table 1 Relative energies of the crucial intermediates in the 'standard' isomerization mechanism (see Fig. 1d), for the ethylene/methyl acrylate copolymerization and ethylene homolpolymerization catalyzed by the Pd-diimine and Ni-diimine catalysts

Species	Relative energy(kcal mol^{-1})			
	Copolymerization-Pd	Homopolymerization-Pd	Copolymerization-Ni	Homopolymerization-Ni
6	**6A-Pd** (0.0)	**6E-Pd** (0.0)	**6A-Ni** (0.0)	**6E-Ni** (0.0)
14	**14A-Pd** (7.8)	**14E-Pd** (4.2)	**14A-Ni** (12.9)	**14E-Ni** (10.4)
8	**8A-Pd** (3.1)	**8E-Pd** (−2.0)	**8A-Ni** (0.1)	**8E-Ni** (−2.1)

Table 2 Crucial bond lengths and the corresponding bond-order values (in parantheses) in the agostic complexes **6A**, 6E, **8A**, and 8E (see Fig. 2) with the Pd-diimine and Ni-diimine catalysts

Species	Bond-length [A] (bond-order) M–H_β	Species	Bond-length [A] (bond-order) M–C_α
		C_β–H_β	
6A-Pd	1.74 (0.14)	1.23 (0.73)	2.04 (0.44)
6E-Pd	1.72 (0.15)	1.25 (0.71)	2.06 (0.49)
6A-Ni	1.65 (0.22)	1.20 (0.73)	1.93 (0.69)
6E-Ni	1.64 (0.24)	1.22 (0.72)	1.92 (0.78)
8A-Pd	1.77 (0.13)	1.21 (0.74)	2.05 (0.44)
8E-Pd	1.81 (0.13)	1.19 (0.75)	2.07 (0.48)
8A-Ni	1.64 (0.21)	1.22 (0.73)	1.93 (0.68)
8E-Ni	1.65 (0.24)	1.20 (0.74)	1.94 (0.79)

along the reaction path. It can be observed in Fig. 5b that the formation of the chelating Pd–O bond follows the breaking of the agostic Pd–H bond. At the transition-state region both bonds are broken. Thus, along the isomerization pathway no structure exists in which both bonds discussed are present. It should also be pointed out that the energy profile of Fig. 5a can be almost perfectly described by two parabolae intersecting at TS. A parabolic fit of calculated energies is characterized by an R^2 value of 0.999. These two harmonic potentials correspond to the Pd–H bond-breaking and the Pd–O bond forming, respectively.

Thus, it may be concluded that for Pd-catalysts the isomerization mechanism in the polar copolymerization is similar to that of homopolymerization, without direct participation of the polar group. The presence of the polar-group increases the isomerization activation barrier and the energy of the intermediate hydride complex.

Isomerization reactions with the Ni-based diimine catalyst

The energy profile for the isomerization process obtained for the species with the polar group and the Ni-diimine catalyst is shown in Fig. 6. The relative energies of the agostic and the π-olefin–hydride complexes are shown in Table 1. As in the case of the Pd-catalyst, there is no direct participation of the polar group in the

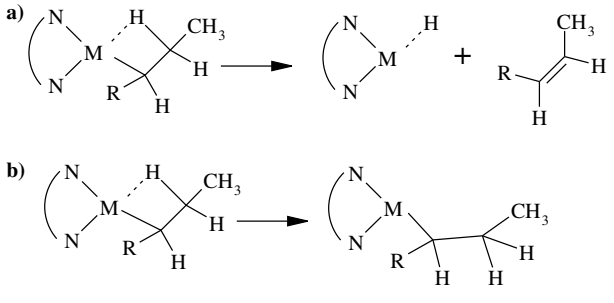

Fig. 4 Reactions used to estimate C_β–H and Pd–C_α bond-energies in the agostic complexes **6A** (see Fig. 2)

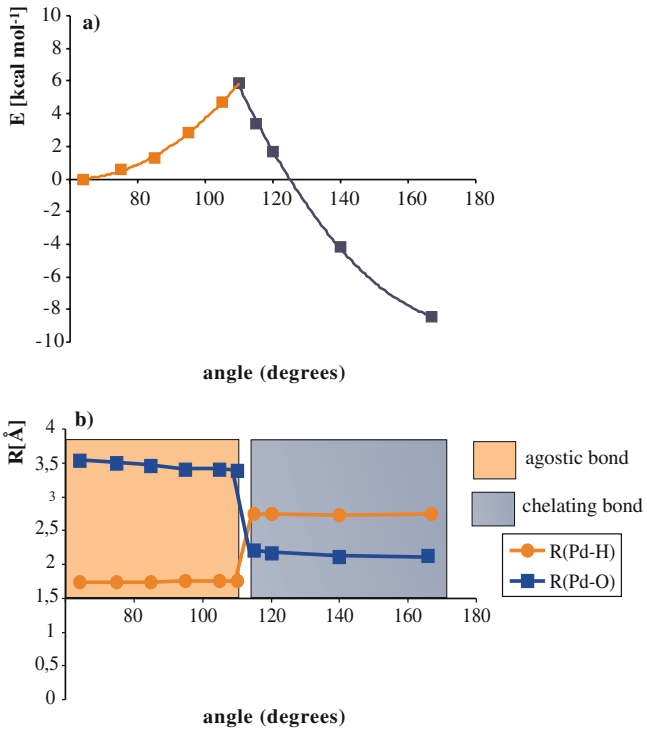

Fig. 5 Energy profile for the agostic ↔ chelate isomerization step, **6A-Pd** ↔ **10A-Pd**, (a) in the process catalyzed by the Pd-diimine catalyst, together with the crucial interatomic distances (b)

isomerization pathway corresponding to that of homopolymerization. There is no Ni–O bond in the agostic complexes (**6A-Ni** and **8A-Ni**), π-olefin–hydride complex (**14A-Ni**), and in the corresponding TS (**6A/14A-Ni**and **14A/8A-Ni**). It is known from earlier experimental and theoretical studies that in the α-olefin homopolymerization with Ni-based catalysts, the isomerization barriers as well as the energies of the intermediate hydride complexes are higher than those with the Pd-catalysts [2, 57–61]. Also, the presence of a polar group leads to an increase in the hydride energies and the activation barriers. Thus, for the Ni-system discussed here both effects can be observed: an increase in the activation barrier and the hydride energy compared to the corresponding palladium-systems, as well as a further increase due to a polar group (see Table 1).

As in the Pd-case, an increase in hydride energy and the isomerization barriers due to a polar group can be explained by a decrease in C_β–H and an increase in Ni–H bond strength. These effects are reflected by corresponding interatomic distances and bond-order indices (Table 2). The C_β–H bond is shortened in **6A-Ni** (1.20 Å) compared to **6E-Ni** (1.22 Å). The corresponding bond-order values are 0.73 and 0.72. In contrast, the Ni–H bond is elongated in **6A-Ni** (1.65 Å) compared to **6E-Ni** (1.64 Å) and the corresponding bond-order values are 0.22 and 0.24. The conclusions from the bond-length /bond-order data are confirmed by calculated bond energies from the dissociation reactions of Fig. 4. The reaction of Fig. 4a (Ni–C and Ni–H bond breaking)

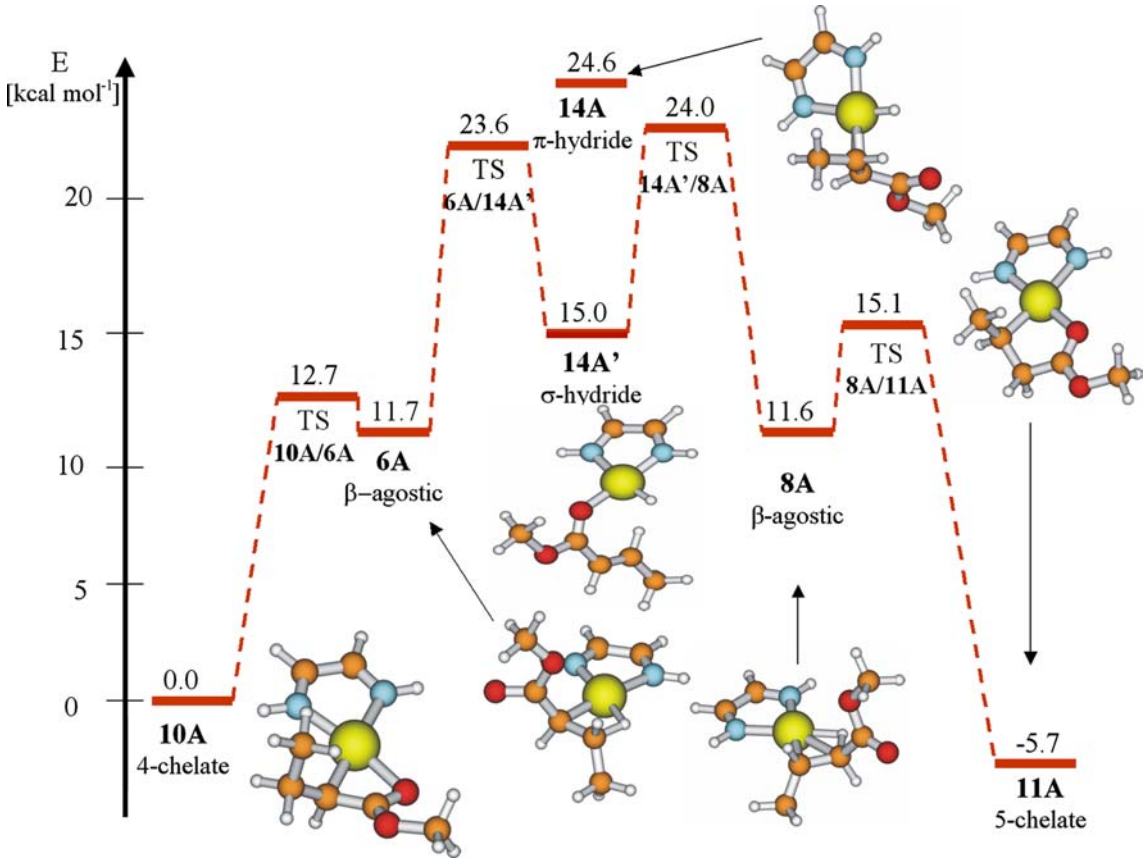

Fig. 6 Energy profile and the crucial structures for the isomerization reactions in the process catalyzed by the Ni-diimine complex. Energies are in kilocalories per mole, structure labelling as in Fig. 2

requires 90.4 kcal mol^{-1} for **6A-Ni** and 89.6 kcal mol^{-1} for **6E-Ni**. Both of these values are larger than for Pd (82.9 and 84.8 kcal mol^{-1}, respectively). The agostic bond energy (Fig. 4b) is 12.2 and 16.0 kcal mol^{-1} for **6A-Ni** and **6E-Ni**, respectively.

Thus, it may be concluded that the polar group effect for the 'standard' isomerization mechanism is an increase in the hydride energies and the activation barriers. However, there is an additional important factor that must be taken into account in a discussion of the isomerization mechanism for the Ni-system. Namely, as an alternative to the hydride–olefin π-complex (**14A**), the hydride–olefin σ-complex (**14A'**) can be formed, with the olefin coordinated to the metal by the oxygen atom of the polar group. This is analogous to the alkyl–olefin complexes. It is known from the previous studies that both, π-binding and σ-binding modes can be observed, and for the Pd-diimine catalyst the former has lower energy, while for the Ni-system the latter is preferred [19, 20]. A preference for the σ-binding mode also well obtained from the calculations for olefin–alkyl complexes with nitrogen-containing monomers [29]. Figure 6 shows that a similar preference of the σ-binding mode occurs here for the hydride–olefin isomerization intermediate with the Ni-catalyst. The σ-olefin–hydride (**14A' -Ni**) is only 3.3 kcal mol^{-1} higher in energy than the agostic species **6A-Ni**, while the π-binding mode (**14A-Ni**) is higher by 12.9 kcal mol^{-1} than **6A-Ni**. Thus, the σ-olefin–hydride complex **14A' -Ni** is 9.6 kcal mol^{-1} lower in energy than the π-olefin–hydride complex **14A-Ni**. It should be pointed out here that for the palladium catalyst the corresponding σ-olefin–hydride complex **14A' -Pd** is 2.6 kcal mol^{-1} higher in energy than the π-olefin–hydride complex **14A-Pd** (Fig. 3).

Results of the Ziegler–Rauk bond-energy decomposition performed for the olefin binding energy in the π-olefin–hydride (**14A**) and the σ-olefin–hydride (**14A'**) complexes with Pd-diimine and Ni-diimine catalysts are shown in Table 3. The results show that the preference of the σ-binding mode observed for the Ni-catalyst comes from the steric and geometry distortion contributions. There is only a small difference in the orbital-interaction terms (below 1 kcal mol^{-1}). This is in agreement with previous results obtained for the σ-olefin–alkyl and π-olefin–alkyl complexes, for which a preference of the σ-mode for Ni-catalysts was attributed to the electrostatic contributions, practically without a difference in the orbital-interaction terms/Fukui function [19, 20].

Thus, in the case of the Ni-catalyst the isomerization mechanism is in fact modified by the presence of the polar group. The pathway involving a σ-olefin–hydride

Table 3 Ziegler–Rauk bond-energy decomposition for the π-olefin–hydride (**14A**) and the σ-olefin–hydride (**14A'**) complexes with the Pd-diimine and Ni-diimine complexes; to facilitate a comparison the difference in respective contributions between the two binding modes are listed in the ΔE column

	14A-Pd	**14A' -Pd**	**ΔE** (kcal mol^{-1})	**14A-Ni**	**14A' -Ni**	**ΔE** (kcal mol^{-1})
ΔE^{a}_{orb}	−64.7	−41.9	−22.8	−64.8	−42.9	−21.9
ΔE^{b}_{st}	21.1	−0.9	22.0	18.8	−8.6	27.4
ΔE^{c}_{dist}	−23.05	−21.3	−1.75	0.8	−2.9	3.7
ΔE^{d}_{total}	−66.65	−64.1	−2.6	−45.5	−54.4	9.2

[a] Orbital-interaction term [b] Steric (electrostatic + Pauli repulsion) term [c] Geometry distortion term [d] Total binding energy

structure is more facile than the 'standard' pathway with a π-olefin–hydride intermediate. For the Ni-catalyst, the activation barrier of such an isomerization (12.3 kcal mol^{-1} with respect to **6A-Ni**), calculated with respect to an agostic complex, is similar to the activation barrier of the 'standard' isomerization observed for the Pd-system (12.5 kcal mol^{-1} with respect to **6A-Pd**). However, comparing the whole isomerization profile, starting from the 4-member chelate and leading to the 5-member chelate, the isomerization is substantially slower in the

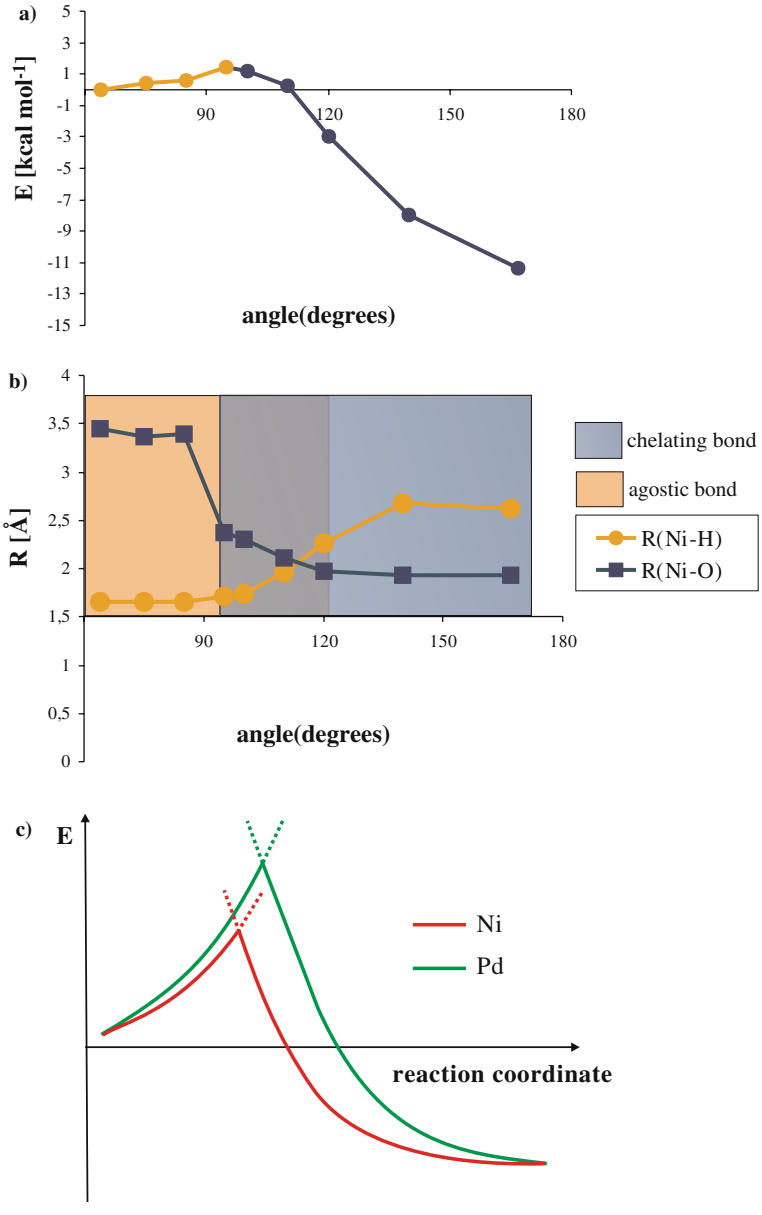

Fig. 7 Energy profile for the agostic ↔ chelate isomerization step, **6A-Ni** ↔ **10A-Ni**, (a) in the process catalyzed by the Ni-diimine catalyst, together with the crucial interatomic distances (b). Origin of a decrease in the activation barrier observed for Ni-catalyst compared to Pd-system is schematically explained in (c)

case of the Ni-based system. The highest transition state energies are 20.9 and 24.0 kcal mol^{-1} (with respect to the 4-member chelate) for the Pd-catalysts and Ni-catalysts, respectively.

Finally, let us discuss the agostic ↔ chelate isomerization (**6A** ↔ 10A) for the Ni-catalyst. The energy profile for this reaction and the changes in the crucial bond-lengths are shown in Fig. 7. The results show that in the Ni-case there is almost no barrier for this reaction. In contrast to the palladium-system, the chelating Ni–O interaction appears before the agostic bond is broken (Fig. 7b). Thus, in the TS-region structures with both Pd–H and Pd–O (partial) bonds exist. This may further modify the mechanism of the isomerization in the Ni-case at higher temperatures, e.g. leading directly to the 5-membered chelate **11A** . Investigating this aspect, however, requires extensive MD studies, and is beyond the scope of this article. The existence of both Pd–H and Pd–O bonds in the TS region is responsible for aforementioned decrease in the agostic ↔ chelate isomerization barrier. It has been pointed out in the previous section that this barrier appears as the result of the intersection of the harmonic potentials describing the Pd–H and Pd–O bond-formation/bond-breaking (Fig. 5). The change in the M–O force constant in the Ni-system compared to Pd is mostly responsible for the barrier disappearing (Fig. 7c). This is confirmed by the value of the reaction coordinate (torsion angle) at the TS state 95^o for Ni, and 110^o for Pd.

Concluding remarks

In the present article isomerization reactions in the polar co-polymerization process catalyzed by the Pd-diimine and Ni-diimine catalysts were studied. This study focused on the influence of the polar group and of the metal in the catalyst on the isomerization mechanism and its energy profile. The results show that for the Pd-based catalyst, the polar group does not influence the mechanism. The isomerization follows the route known from the ethylene homopolymerization. It involves β-hydrogen transfer to the metal with formation of the π-olefin–hydride intermediate complex. The electron-withdrawing character of the polar group results in the C_β–H bond strengthening accompanied by weakening of the Pd–H interaction. These factors are responsible for an increase in the relative energy of the hydride complex and the isomerization TS. In the corresponding mechanism for the Ni-catalyst, the hydride energy and the activation barriers are increased compared to Pd-systems. However, in the Ni-case the polar group affects the mechanism by formation of an alternative hydride complex with the olefin bound by the carbonyl oxygen (σ-complex). Such a species has lower energy than the π-olefin hydride. This is similar to the σ-complex preference observed for alkyl–olefin complexes for the Ni-catalyst [19, 20]. Thus, comparing the whole isomerization profile, starting from the 4-membered chelate and leading to the 5-membered chelate, the highest transition state energies are 20.9 and 24.0 kcal mol^{-1} (with respect to the 4-member chelate) for the Pd-catalysts and Ni-catalysts, respectively. This indicates that the isomerization is substantially slower in the case of the Ni-based system. This can result in a larger fraction of ester group directly connected to the copolymer backbone and of those located in shorter branches. This is in a qualitative agreement with available experimental data. For Ni-catalysts predominantly in-chain acrylate incorporation was observed [25], while for Pd-catalysts the ester groups occur largely at the ends of branches [2, 7, 8, 25].

References

1. Britovsek GJP, Gibson VC, Wass DF (1999) Angew Chem Int E 38:428–447 (references therein)
2. Ittel SD, Johnson LK, Brookhart M (2000) (references therein). Chem Rev 100:1169–1203
3. Gibson VC, Spitzmesser SK (2003) (references therein). Chem Rev 103:283–315
4. Patil AO, Hlatky GG (eds) (2003) Beyond metallocenes. Next-generation polymerization catalysts. ACS Symposium Series 857, American Chemical Society, Washington, DC (references therein)
5. Hermann WA, Cornilis B (1997) (references therein). Angew Chem Int 36:1048–1067
6. Boffa LS, Novak BM (2000) (references therein). Chem Rev 100:1479–1494
7. Johnson LK, Mecking S, Brookhart M (1996) J Am Chem Soc 118:267–268
8. Mecking S, Johnson LK, Wang L, Brookhart M (1998) J Am Chem Soc 120:888–899
9. Johnson LK, Killian CM, Brookhart M (1995) J Am Chem Soc 117:6414–6415
10. Killian CM, Tempel DJ, Johnson LK, Brookhart M (1996) J Am Chem Soc 118:11664–11665
11. Guan Z, Cotts PM, McCord EF, McLain SJ (1999) Science 283:2059–2062
12. Cotts PM, Guan Z, McCord EF, McLain SJ (2000) Macromolecules 33:6945–6952
13. Gates DP, Svejda SA, Onate E, Killian CM, Johnson LK, White PS, Brookhart M (2000) Macromolecules 33:2320–2334
14. McCord EF, McLain SJ, Nelson LTJ, Arthur SD, Coughlin EB, Ittel SD, Johnson LK, Tempel D, Killian CM, Brookhart M (2001) Macromolecules 34:362–371
15. Michalak A, Ziegler T (2002) J Am Chem Soc 124:7519–7528
16. Michalak A, Ziegler T (2003) Macromolecules 36:928–933
17. Cossee P (1964) J Catal 3:80–88
18. Arlman EJ, Cossee P (1964) J Catal 3:99–104
19. Michalak A, Ziegler T (2001) Organometallics 20:1521–1532
20. Michalak A (2004) Chem Phys Lett 386:346–350
21. Michalak A, Ziegler T (1999) Organometallics 18:3998–4004
22. Michalak A, Ziegler T (2000) Organometallics 19:1850–1858
23. Michalak A, Ziegler T (2001) J Am Chem Soc 123:12266–12278
24. Michalak A, Ziegler T (2003) Organometallics 22:26602669
25. Johnson L, Wang L, McLain S, Bennett A, Dobbs K, Hauptman E, Ionkin A, Ittel S, Kunitsky K, Marshall W, McCord E, Radzewich C, Rinehart A, Sweetman KJ, Wang Y, Yin Z, Brookhart M (2003) Copolymerization of ethylene and acrylates by nickel catalysts. In: Patil AO, Hlatky GG (eds) Beyond metallocenes. Next-generation polymerization catalysts. ACS Symposium Series 857, American Chemical Society, Washington, DC, pp131–142
26. Maseras F, Lledos A (eds) (2002) Computational modeling of homogeneous catalysis (references therein). Kluwer Academic Publishers, Dordrecht

27. Rappe AK, Skiff WM, Casewit CJ (2000) (references therein). Chem Rev 100:1435–1456
28. Angermund K, Fink G, Jensen VR, Kleinschmidt R (2000) (references therein). Chem Rev 100:1457–1470
29. Deubel DV, Ziegler T (2002) Organometallics 21:1603–1611
30. Deubel DV, Ziegler T (2002) Organometallics 21:4432–4441
31. Schenck H, Stromberg S, Zetterberg K, Ludwig M, Akermark B, Svensson M (2001) Organometallics 20:2813–2819
32. Phillip DM, Muller RP, Goddard WA, Storer J, McAdon M, Mullis M (2002) J Am Chem Soc 124:10198–10210
33. Frenking G, Frohlich N (2000) (references therein). Chem Rev 100:717–774
34. Cundari TR (2000) (references therein). Chem Rev 100:807–818
35. Dedieu A (2000) Chem Rev 100:543–600
36. Niu S, Hall MB (2000) (references therein). Chem Rev 100:353–406
37. Becke A (1988) Phys Rev A 38:3098–3100
38. Perdew JP (1986) Phys Rev B 34:7406–7406
39. Perdew JP (1986) Phys Rev B 33:8822–8824
40. TeVelde G, Bickelhaupt FM, Baerends EJ, Fonseca Guerra C, van Gisbergen SJA, Snijders JG, Ziegler T (2001) (references therein). J Comput Chem 22:931–967
41. Baerends EJ, Ellis DE, Ros P (1973) Chem Phys 2:41–51
42. Boerrigter PM, te Velde G, Baerends EJ (1988) Int J Quantum Chem 33:87–113
43. Versluis L, Ziegler T (1988) J Chem Phys 88:322–328
44. te Velde G, Baerends EJ (1992) J Comput Phys 99:84–98
45. Fonesca Geurra C, Visser O, Snijders JG, te Velde G, Baerends EJ (1995) In: Clementi E, Corongiu G (eds) Methods and techniques in computational chemistry METACC-9. STEF, Cagliari, pp. 303–395
46. Ziegler T, Tschinke V, Baerends EJ, Snijders JG, Ravenek W (1989) J Phys Chem 93:3050–3056
47. Snijders JG, Baerends E (1978) Mol Phys 36:1789–1904
48. Snijders JG, Baerends EJ, Ros P (1979) Mol Phys 38:1909–1929
49. Deng L, Ziegler T, Woo TK, Margl P, Fan T (1998) Organometallics 17:3240–3253
50. Nalewajski RF, Mrozek J, Formosinho SJ, Varandas AJC (1994) Int J Quantum Chem 52:1153–1176
51. Nalewajski RF, Mrozek J (1994) Int J Quantum Chem 51:187–200
52. Nalewajski RF, Mrozek J, Mazur G (1996) Can J Chem 74:1121–1130
53. Nalewajski RF, Mrozek J, Michalak A (1997) Int J Quantum Chem 61:589–601
54. Nalewajski RF, Mrozek J, Michalak A (1998) Pol J Chem 72:1779–1791
55. Ziegler T, Rauk A (1978) Theor Chim Acta 46:1–9
56. Ziegler T, Rauk A (1979) Inorg Chem 18:1755–1759
57. Musaev DG, Froese RDJ, Morokuma K (1998) Organometallics 17:1850–1860
58. Froese RDJ, Musaev DG, Morokuma K (1998) J Am Chem Soc 120:1581–1587
59. Deng L, Margl P, Ziegler T (1997) J Am Chem Soc 119:1094–1100
60. Deng L, Woo TK, Cavallo L, Margl PM, Ziegler T (1997) J Am Chem Soc 119:6177–6186
61. Leatherman MD, Svejda SA, Johnson LK, Brookhart M (2003) J Am Chem Soc 125:3068–3081